Journal of Fluorescence (2019) 29:1007–1012
https://doi.org/10.1007/s10895-019-02414-z

ORIGINAL ARTICLE

Proton Beam Induced Modification of Luminescence Properties of Polystyrene/Al_2O_3 Polymer Nanocomposites

Shilpa Bhavsar [1] · **N. L. Singh** [1] · **S. V. Suryanarayana** [2] · **K. V. R. Murthy** [3]

Received: 17 May 2019 / Accepted: 3 July 2019 / Published online: 10 July 2019

Abstract
Polystyrene polymer (PS)/Al_2O_3 nanocomposite films were synthesized from PS:Al_2O_3 (1–x):x mixtures (x = 3 wt%) via solution casting method. These nanocomposite films were exposed to 5 MeV proton beam of different fluences. The proton beam induced changes in optical and luminescence properties of PS and PS:Al_2O_3 films have been investigated using FTIR, UV-visible, Photoluminescence and thermoluminescence studies. FTIR studies concede reduction in the peak intensity due to doping of Al_2O_3 and proton irradiation. The UV-visible spectra show shifting of absorption edge with increasing fluence. This can be attributed to creation of conjugated system of bonds. The band gap of PS and 3 wt% Al_2O_3 doped PS is observed to be 4.38 eV and 4.34 eV, respectively, whereas the band gaps of proton irradiated 3 wt% Al_2O_3 doped PS films are found to be 4.28 eV and 4.23 eV at the fluences of 1×10^{12} ions/cm^2 and 1×10^{13} ions/cm^2, respectively. The photoluminescence emission spectra show three peaks, wavelength at 411 nm, 435 nm and 462 nm corresponding to the PS in violet-blue region when excited with near UV wavelength of 380 nm. The intensity of emission peaks was found to increase with increasing fluence. The thermoluminescence curves of PS/Al_2O_3 were analysed using glow curve deconvolution method (GCD). The increase in TL peak intensity of the glow curve was observed as fluence increase.

Keywords Polymer nanocomposites · Proton irradiation · Photoluminescence · Thermoluminescence

Introduction

Properties of both the inorganic and organic nanocomposite materials have been receiving intense attention over past many years due to their wide ranging applications such as in opto-electronic device, high efficiency electrochemical device, coating, packaging, fibers and such other applications [1–3]. Among the wide variety of polymers available, polystyrene (PS) is one of the most popular and widely-used polymers because of its excellent transparency, processability and bio-compatibility [4]. In contrast to the traditional polymer composites with micron size dopants, introduction of nano-scale fillers into polymer matrix causes reduced distance between filler particles by increasing their number density. Addition of nanoparticles like ZrO_2, ZnO, SiO_2, TiO_2 and Al_2O_3 into polymer matrices significantly improved the polymer properties, like mechanical strength, toughness, electrical and thermal conductivities and optical properties because of strong interfacial interaction between the polymer and the nanoparticles [5].

In particular, aluminum oxide NPs (nanoparticles) have many attractive properties such as good thermal conductivity, high mechanical strength and stiffness, high adsorption capacity, wear resistance, thermal stability and abrasiveness. Moreover, it is also inexpensive and non-toxic [6, 7]. Similar method is used for acquiring polymer composites or nanocomposites by employing the micron and nanoparticles such as CdS, Eu_2O_3, Al_2O_3, SiO_2 etc. with polystyrene [4, 8–10]. It is found upon the literature survey that there are quite a few reports available, on enhancement of luminescence properties of polystyrene based polymer nanocomposites modified with proton beam irradiation. Proton beam irradiation of polymer nanocomposite is a unique approach to produce active sites

✉ Shilpa Bhavsar
bhavsar.shilpa212@gmail.com

1 Department of Physics, The M. S. University of Baroda, Gujarat 390002, India

2 Nuclear Physics Division, Bhabha Atomic Research Centre, Mumbai 400 085, India

3 Department of Applied Physics, The M. S. University of Baroda, Gujarat 390002, India

which can cause irreversible changes in physical and chemical properties of the polymer nanocomposites by electronic excitation and ionization in a controlled way.

The aim of present work is to study effect of proton beam irradiation on optical and luminescence properties of 3 wt% Al_2O_3 doped PS. The investigation was carried out using UV-visible spectroscopy, photoluminescence and thermoluminescence measurements on films irradiated at different proton beam fluences.

Experimental Details

Materials

The polystyrene was obtained from National Laboratory. Al_2O_3 (99.99%) of size less than 50 nm was obtained from Sigma Aldrich. Toluene (99.5%) used as the solvent was purchased from Suvidhnath Laboratories. All chemicals were of AR Grade.

Preparation of PS/Al_2O_3 Films

The $PS_{100-x}(Al_2O_3)_x$ (x = 3 wt%) polymer nanocomposite film was prepared using solution casting method. An appropriate amount of PS granules was dissolved in toluene until a clear solution appeared, followed by dispersion of 3 wt% Al_2O_3 in the solution. The mixture was stirred continuously for 24 h at room temperature using magnetic stirrer. The solution was then poured into petri dishes and kept aside until solvent-free films were formed. The thickness of the films obtained was around 120 μm. The above procedure is followed to prepare, 3 wt% Al_2O_3 doped PS films (pristine) labelled as PA3.

Proton Beam Irradiation of PA3 Films

Self-standing PA3 films were irradiated with proton beam of fluences of 1×10^{12} ions/cm^2 and 1×10^{13} ions/cm^2 with a current of 2 nA at BARC, Mumbai. SRIM-2008 code was used to calculate the projectile range, electronic energy loss and nuclear energy loss of the 5 MeV proton beam. The value of projectile range, electronic energy loss and nuclear energy loss was found to be 335.29 μm, 8.469 keV per micron and 4.969×10^{-3} keV per micron, respectively.

Characterization of PS-Al_2O_3 Nanocomposite Films

The X-Ray diffraction patterns of PS and PA3 were acquired using Bruker D8-Advance Diffractometer with wavelength λ = 1.5418 Å and were recorded in the range of Bragg angle 2 from 10° to 50°. FTIR spectra of pristine and irradiated samples were recorded using JASCO-4100 spectrometer. The UV-visible analysis was carried out using Hitachi Model U-3300 spectrometer in 200–700 nm wavelength range, while the PL spectra were recorded with the help of Shimadzu Spectrofluorophotometer (1503R-PC). The PL excitation and emission analyses were carried out in the wavelength ranges 220–400 nm and 400–550 nm, respectively. The TL measurements were carried out using Harshaw-3500 TLD Reader with a heating rate of 3 K/S.

Results & Discussion

XRD Analysis

The X-ray diffraction patterns of pristine PS, PA3 and PA3 irradiated are shown in Fig. 1a. Figure 1b is the XRD pattern of Al_2O_3 nanoparticles. The diffraction peaks of Al_2O_3 nanoparticles are observed around 2 = 20.27, 32.00, 37.03, 40.18, 45.65, 60.3 and 66.85 indexed as (111), (220), (311), (222), (400), (511) and (440), respectively, which comply with FCC structure of Al_2O_3 (JCPDS -29-0063). The diffraction peak of PS was observed around 2 = 19.5°. The intensity of the PS

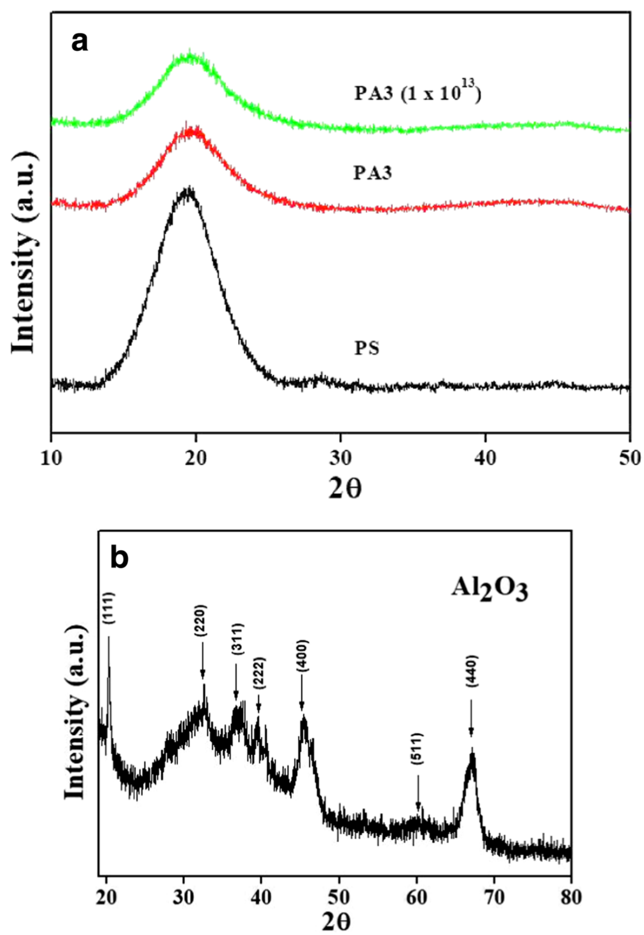

Fig. 1 XRD spectra of (**a**) pristine PS and pristine and irradiated PA3 (**b**) Al_2O_3

peak shows a decrease due to incorporation of 3 wt% nanoparticles. On the other hand, no observable change in the XRD peak of PA3 after irradiation was noted, implying no structural change in PA3 due to proton beam irradiation.

FTIR Analysis

Figure 2 illustrates FTIR spectra of pristine and irradiated polymer nanocomposites. The various functional groups related to PS structure are classified as follows: (a) C=C stretching mode observed at 1488.7 and 1604.3 cm^{-1}. (b) The band at 3061 and 3090.2 cm^{-1} are assigned to C-H stretching mode in phenyl ring. (c) The band observed in the range of 3000–2800 cm^{-1} attributed to C-H bond stretching of saturated alkane. It has been seen that due to incorporation of filler, new peak have been seen at 1641 and 1703.8 cm^{-1}, ascribed to Al-O group of Al_2O_3 and C=O stretching vibration, respectively. This result confirms the presence of Al_2O_3. The observed decrease in the intensity of peak corresponding to the PS (as mentioned above) is due to incorporation of filler and proton irradiation. The band in the range 675–950 cm^{-1} (C-H bending vibration) completely disappears at the fluence of 1×10^{13} ions/cm^2. These results are a consequence of occurrence of chain scissioning or crosslinking of polymer matrix due to proton irradiation.

UV-Visible Spectral Analysis

The UV-vis spectra of pristine PS, PA3 and PA3 irradiated with 5 MeV proton beam are depicted in Fig. 3. The absorption edge are corresponding to π-π* transition and are related

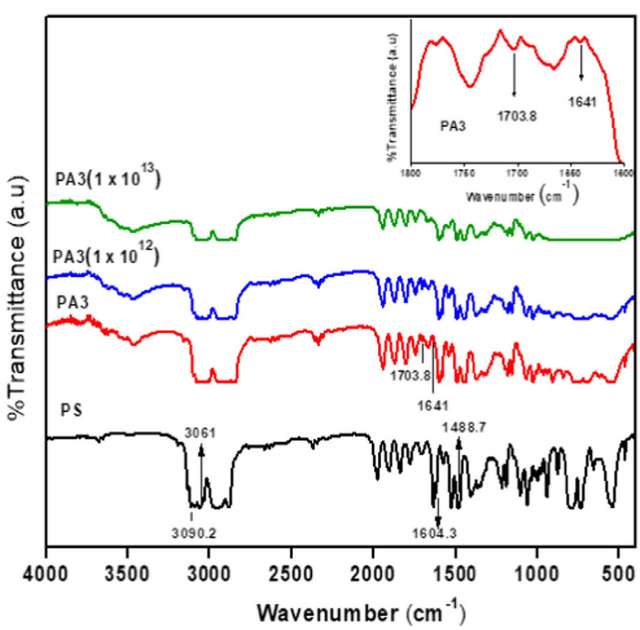

Fig. 2 FTIR spectra of pristine PS and pristine and irradiated PA3 (inset: magnified image of pristine PA3 in the range of 1600–1800 cm^{-1})

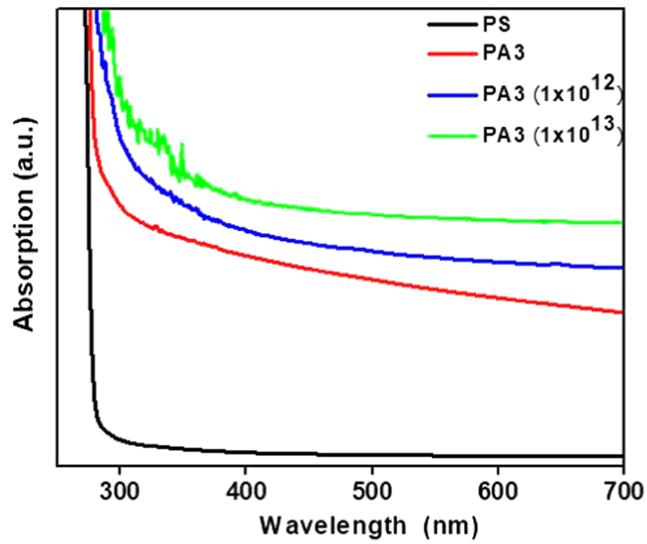

Fig. 3 UV-visible spectra of PS and pristine and irradiated PA3

to phenyl ring having C=C and C=O double bonds. The figure shows shift of absorption edge towards longer wavelength with increasing fluence. This can be ascribed to formation of conjugated system of double and triple bonds owing to few rupture and reconstruction of bonds. In addition, the absorption edge has become broader with increasing fluence indicating creation of defects as well as low molecular weight radicals and ions [11]. The direct band gaps of pristine and irradiated polymer nanocomposites are determined using Tauc's relation [12]:

$$\alpha h\nu = B\left(h\nu - E_g\right)^{\frac{1}{2}}$$

where α and B are the absorption coefficient and a constant, respectively. The band gap (E_g) was obtained using $(\alpha h\nu)^2$ versus the photon energy ($h\nu$) plot. The straight line region of the plot on higher energy side when extrapolated to $\alpha = 0$, the photon energy intercept gives the band gap [12]. The band gap values obtained are shown in Table 1. The band gap of PA3 is observed to decrease with increasing ion fluence. This decrease in band gap implies formation of carbon enriched domains with reduction of H/C ratio as a result of crosslinking of polymer chains. This is due to formation of radicals and evolution of hydrogen during proton irradiation. After

Table 1 Band gap of pristine and irradiated PA3 nanocomposite films

Sample	Band Gap 'E_g' (eV)
PS	4.38
PA3	4.34
PA3 (1×10^{12})	4.28
PA3 (1×10^{13})	4.23

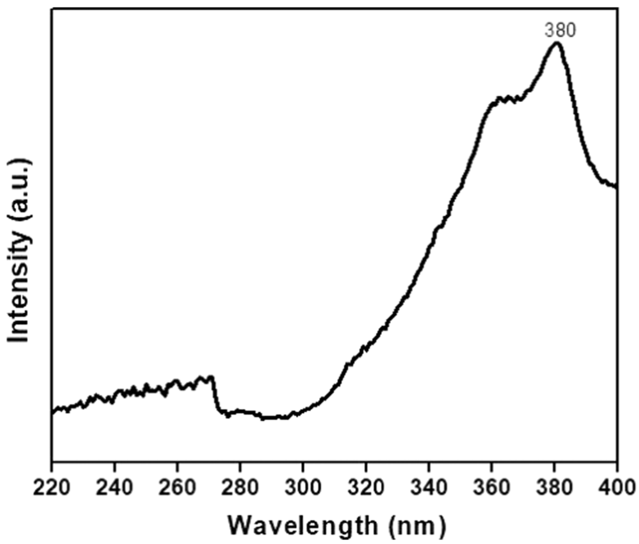

Fig. 4 Photoluminescence excitation spectra of PS monitored at 435 nm

irradiation, the colour of the films was observed to change to brown from being transparent. This can be ascribed to formation of unsaturated bonds. These bonds have abundant amount of charge carriers and require less energy to assist electronic transition from HOMO to LUMO bands [13] (Fig. 4).

Photoluminescence Study

Figure 5 shows PL emission spectra of pristine PS and pristine and irradiated PA3 films. The peak profile of irradiated PA3 is the same as of pristine PA3. It is seen that broad peaks at wavelength 411 nm, 435 nm and 462 nm observed in emission spectra of PS with excitation wavelength 380 nm while photoluminescence excitation spectrum was recorded with emission wavelength monitored at 435 nm as shown in Fig. 4. The intensity of PL emission spectra of irradiated PA3 is observed to increase compared to that of pristine PA3

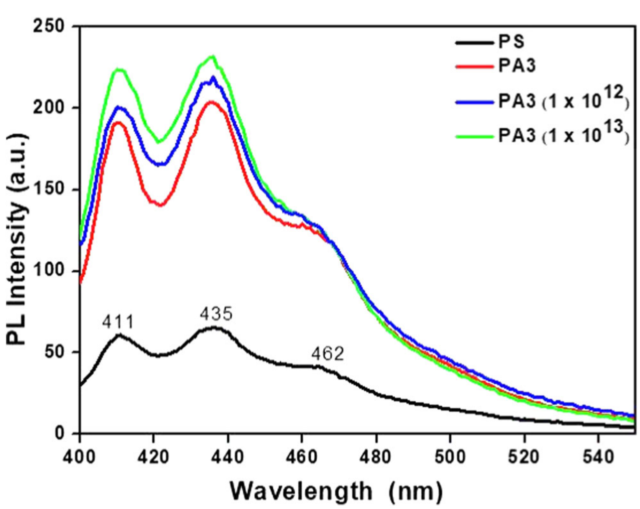

Fig. 5 Photoluminescence emission spectra of pristine and irradiated samples with excitation wavelength 380 nm

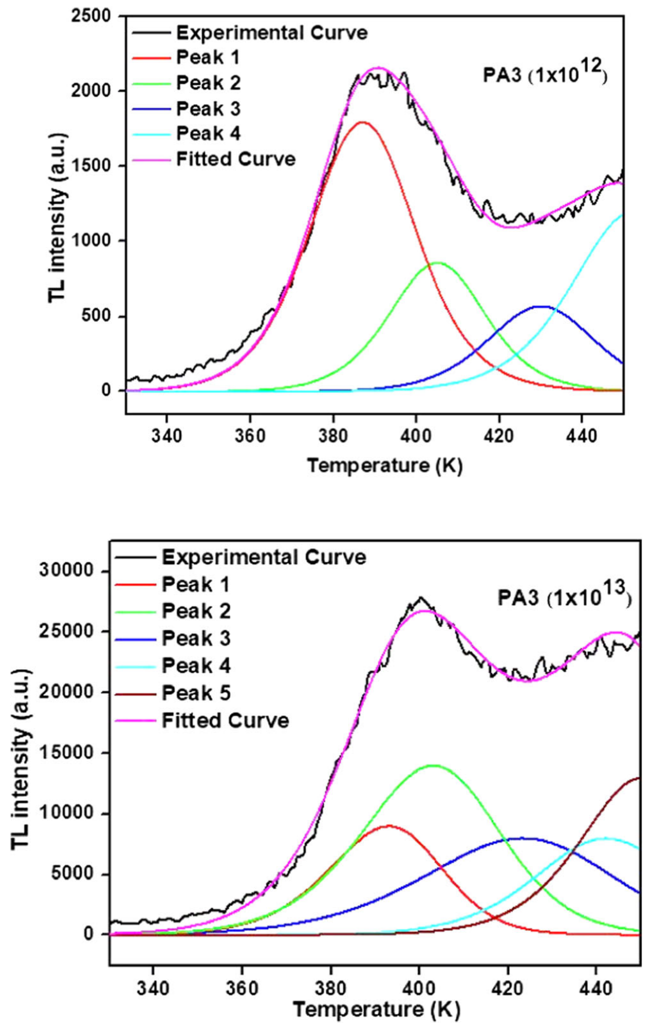

Fig. 6 Thermoluminescence glow curve of irradiated PA3

sample. The augmentation of PL intensity upon irradiation is due to creation of radiative recombination levels which can be associated with ion prompted modification in the configuration of the facial layer [14]. This might be owing to change in microstructure of PS and relocation of Al_2O_3 nanoparticles in

Table 2 The value of activation energy E_a and b are calculated from GCD method for irradiated PA3 films of different fluences

Samples	Curve	E_a (eV)	*b*	*s* (s^{-1})
PA3 (1×10^{12})	1	1.655	1.8	2.3×10^{17}
	2	1.365	1.8	5.8×10^{19}
	3	1.674	1.8	3.7×10^{19}
	4	1.54	1.43	2.0×10^{22}
PA3 (1×10^{13})	1	0.84	1.419	2.5×10^{9}
	2	1.26	1.47	1.0×10^{15}
	3	1.1	1.54	4.5×10^{11}
	4	1.42	1.8	8.0×10^{14}
	5	1.61	1.4	4.1×10^{15}

PS film through creation of tracks in PA3 after proton irradiation [15]. This is due to cleavage of carbonate bonds with extraction of hydrogen from side group as well as main chain of the polymer during proton irradiation. These results suggest formation of polycyclic aromatic hydrocarbons [16]. Moreover, the shifting of the emission peak at 411 nm towards longer wavelength implies formation of defects or prevention of chemical species by increasing evolution of energy during irradiation [14]. This result was correlated with the UV-visible and FTIR spectra result. Thus PA3 may prove to be a potential candidate for LED applications when excited with 380 nm.

Thermoluminescence Study

The thermoluminescence glow curves of PS/Al_2O_3 polymer nanocomposites are shown in Fig. 6. The TL glow curves are fitted with deconvolution method which is used to analyse the curves and calculate the attendant kinetic parameters. Large variation in the value of activation energy found corresponds to continuous distribution of traps.

Due to complex nature of the glow curves of PS/Al_2O_3 polymer nanocomposites, the glow curve deconvolution method is more convenient for the analysis. The glow curve parameters, namely, kinetic parameters and activation energy are calculated using glow curve deconvolution using mixed order kinetics model given by Kitis et al.:

$$I(T) = \mathrm{Im} b^{b-1} \exp\left(\frac{E}{kT} x \frac{T-Tm}{Tm}\right)$$
$$x\left((b-1)\frac{T^2}{Tm^2}\left(1-\frac{2kT}{E}\right)\exp\left(\frac{E}{kT} x \frac{T-Tm}{Tm}\right)+1+(b-1)\frac{2kTm}{E}\right)^{-\frac{b}{b-1}}$$

where $I(T)$ is the rate of production of emitted photons or intensity, E_a is the activation energy, k and b are the Boltzmann's constant and the order of kinetics respectively [17]. The value of b corresponds to the general order TL mechanism. GCD method is suitable for calculating the value of activation energy of traps. Calculated values of E_a, b and s are listed in Table 2.

The glow curves of PA3 are broader in the region 386 K to 398 K and exhibit several overlapping peaks. The glow curves corresponding to the polymer composites may be described through the chain scissioning/crosslinking, fragmentation of radical, excitation and dissociation of dopant and creation of charged species through proton beam irradiation which may be a consequence for trapping of charge carriers. The trapped charge carriers are liberated by molecular motion of polymer segment during heating. These liberated charge carriers are recombined by dissipating energy in the form of light. The temperature range of TL glow curve indicates that, during heating, the charge carriers are released from trapping sites due to β relaxations of PS chain, i.e., the rotation of phenyl groups of PS [18]. The intensity of glow curves increases with increasing fluence implying related free electrons from traps [19].

Conclusion

Polymer nanocomposites based on polystyrene and Al_2O_3 nanoparticles were successfully synthesized using solution casting method. The films obtained were irradiated with 5 MeV proton beam at different fluences and at ambient temperature. The FTIR spectra show decrease in the band intensity due to proton irradiation, caused by chain scissioning/crosslinking. After proton beam irradiation, the decrease in band gap and increase in photoluminescence intensity are due to creation of polycyclic aromatic hydrocarbon. This result also indicates promotion of radiative process and defects due to proton beam irradiation. Looking to the overall PL results, PA3 may be useful in semiconductor LED applications using excitation wavelength of 380 nm. This investigation indicates that the luminescence properties of PS/Al_2O_3 get intensified by 5 MeV proton beam irradiation. The TL glow curves of PA3 are owing to the rotation of phenyl group of PS and introduction of defects in PS which was induced due to proton beam irradiation. The activation energy and frequency factor of TL glow curves are found in the range 0.84–1.674 eV and 10^9 - 10^{22} s^{-1}, respectively.

Acknowledgements The financial support provided by IUAC, New Delhi is also gratefully acknowledged. Authors are thankful to Dr. Balak Das, Dept. of Physics, University of Lucknow for providing XRD measurement.

References

1. Jeeju PP, Jayalekshmi S, Chandrasekharan K, Sudheesh P (2012) Size dependent nonlinear optical properties of spin coated zinc oxide-polystyrene nanocomposite films. Opt Commun 285:5433–5439. https://doi.org/10.1016/j.tsf.2012.12.043
2. Elashmawi IS, Hakeem NA, Marei LK, Hanna FF (2010) Structure and performance of ZnO/PVC nanocomposites. Phys B Condens Matter 405:4163–4169. https://doi.org/10.1016/j.physb.2010.07.006
3. Fernandes DM, Hechenleitner AA, Lima SM, Andrade LH, Caires AR, Gómez Pineda EA (2011) Preparation, characterization, and photoluminescence study of PVA/ZnO nanocomposite films. Mater Chem Phys 128:371–376. https://doi.org/10.1016/j.matchemphys.2011.03.002
4. Tripathi SK, Kaur R, Jyoti (2015) Investigation of non-linear optical properties of CdS/PS polymer nanocomposite synthesized by chemical route. Opt Commun 352:55–62. https://doi.org/10.1016/j.optcom.2015.04.042
5. Maji P, Choudhary RB, Majhi M (2016) Structural, optical and dielectric properties of ZrO_2 reinforced polymeric nanocomposite films of polymethylmethacrylate (PMMA). Optik 127:4848–4853. https://doi.org/10.1016/j.ijleo.2016.02.025
6. Karlsson M, Palsgard E, Wilshaw PR, Silvio LD (2003) Initial in vitro interaction of osteoblasts with nano-porous alumina. Biomaterials 24:3039–3046. https://doi.org/10.1016/S0142-9612(03)00146-7
7. Zhang Z, Lei H (2008) Preparation of a -alumina / polymethacrylic acid composite abrasive and its CMP performance on glass substrate. Microelectron Eng 85:714–720. https://doi.org/10.1016/j.mee.2008.01.001

8. Bhavsar S, Patel GB, Singh NL (2018) Effect of γ-irradiation on optical properties of Eu_2O_3-doped polystyrene polymer films. Luminescence 33:1243–1248. https://doi.org/10.1002/bio.3541
9. Bhavsar S, Patel GB, Singh NL (2018) Investigation of optical properties of aluminium oxide doped polystyrene polymer nano-composite films. Phys B Condens Matter 533:12–16. https://doi.org/10.1016/j.physb.2017.12.055
10. Baba EM, Cansoy CE, Zayim EO (2016) Investigation of wettability and optical properties of superhydrophobic polystyrene-SiO_2 composite surfaces. Prog Org Coat 99:378–385. https://doi.org/10.1016/j.porgcoat.2016.06.016
11. Patel GB, Singh NL, Singh F (2017) Modification of chitosan-based biodegradable polymer by irradiation with MeV ions for electrolyte applications. Mater Sci Eng B 225:150–159. https://doi.org/10.1016/j.mseb.2017.08.023
12. Tauc J, Grigorovici R, Vancu A (1966) Optical properties and electronic structure of amorphous germanium. Phys Status Solidi 15: 627–637
13. Chahal RP, Mahendia S, Tomar AK, Kumar S (2012) C-irradiated PVA/Ag nanocomposite films: materials for optical application. J Alloys Compd 538:212–219. https://doi.org/10.1016/j.optmat.2015.12.049
14. Bharti ML, Singh F, Ramola RC, Joshi V (2017) Photoluminescence and reflectivity studies of high energy light ions irradiated polymethyl methacrylate films. Opt Mater 73:550–554. https://doi.org/10.1016/j.optmat.2017.09.018
15. Sharma S, Vyas R, Shrivastava S, Vijay YK (2011) Effect of swift heavy ion irradiation on photoluminescence properties of ZnO/PMMA nanocomposite film. Phys B Condens Matter 406:3230–3233. https://doi.org/10.1016/j.physb.2011.05.030
16. Kim E, Kyhm J, Kim JH, Lee GY, Ko DH, Han IK, Ko H (2013) White light emission from polystyrene under pulsed ultra violet laser irradiation. Sci Rep 3:1–4. https://doi.org/10.1038/srep03253
17. Kitis G, Gomez-Ros JM, Tuyn JWN (1998) Thermoluminescence glow-curve deconvolution functions for first, second and general orders of kinetics. J Phys D Appl Phys 31:2636–2641. https://doi.org/10.1088/0022-3727/31/19/037
18. Dobruchowska E, Okrasa L, Glowacki I, Ulanski J, Boiteux G (2004) The " wet dog " effect in polymers as seen by thermoluminescence. Polym. 45:6027–6035. https://doi.org/10.1016/j.polymer.2004.06.019
19. Pender LF, Fleming RJ (1977) Thermoluminescence in polystyrene. J Phys C Solid State Phys 10:1571–1586. https://doi.org/10.1088/0022-3719/10/9/027